Materials Research Bulletin 47 (2012) 3216–3223

Contents lists available at SciVerse ScienceDirect

Materials Research Bulletin

journal homepage: www.elsevier.com/locate/matresbu

Solution phase synthesis of $Na_{0.28}V_2O_5$ nanobelts into nanorings and the electrochemical performance in Li battery

Ganganagappa Nagaraju [a,b,*], Gujjarahalli Thimmanna Chandrappa [b]

[a] Centre for Nano and Materials Science, Jain University, Jakkasandra Post, Kanakapura, India
[b] Department of Chemistry, Central College Campus, Bangalore University, Bangalore, India

ARTICLE INFO

Article history:
Received 8 February 2012
Received in revised form 6 July 2012
Accepted 10 August 2012
Available online 18 August 2012

Keywords:
$Na_{0.28}V_2O_5$ nanorings
Nanobelts
Hydrothermal
Lithium ion battery

ABSTRACT

In this paper, we are the first to report a simple one step hydrothermal method to synthesize $Na_{0.28}V_2O_5$ nanorings/nanobelts without using any organic surfactant/solvents at 130–160 °C for 1–2 days. The obtained products have been characterized by X-ray diffraction (XRD), energy dispersive X-ray spectroscopy (EDS), Fourier transform infrared spectroscopy (FTIR), Raman spectroscopy, morphology by scanning electron microscopy (SEM) and transmission electron microscopy (TEM) and electrochemical discharge–charge test for lithium battery. XRD pattern exhibit a monoclinic $Na_{0.28}V_2O_5$ structure. FTIR spectrum shows band at 958 cm^{-1} is assigned to V=O stretching vibration, which is sensitive to intercalation and suggests that Na^+ ions are inserted between the vanadium oxide layers. TEM analyses reveal that the products consist of nanorings of width about 500 nm and thickness of about 100 nm with inner diameter of 5–7 μm. Nanobelts of width 70–100 nm and several tens of micrometers in length are observed. The electrochemical results show that nanorings/nanobelts exhibit an initial discharge capacity of 320 mAh g^{-1} and its capacity still retained 175 mAh g^{-1} even after 69 cycles. We have discussed the possible growth mechanism for the formation of nanorings/nanobelts.

1. Introduction

The synthesis of size and shape controlled nanostructures is important for the control of their chemical and physical properties and this forms the basis for the design of novel materials, devices and techniques with multiple applications in electronics, catalysis, biotechnology and medicine [1]. Recently, it has been demonstrated that synthesis of several new geometrical configurations with controlled morphology such as nanosprings [2,3], nanorings [2,4–8] and nanohelices [9,10] from 1D nanobelts/nanowires are of special interest owing to their unique periodic and elastic properties resulting in structural flexibility that provides additional opportunities for nanoengineering.

Among the transition-metal oxides, vanadium oxides and their derived nanostructural compounds show particularly rich chemistry because of the tunable vanadium oxidation state and flexible coordination environment [11]. A rich diversity of vanadium oxide bronzes is based on the incorporation of alkali, alkaline or transition metals within the interstitial spaces of the vanadium oxide tunnel framework and which have been extensively studied [12]. Moreover, the properties of pure V_2O_5 were greatly enhanced by the addition of alkali or alkaline-earth metal ions (Li, Na, Mg) into the host vanadium oxide [13–15]. As a member of the aforementioned vanadium-oxide based compounds, $Na_xV_2O_5$ has attract intense research attention as they possess such properties as a charge ordering transition [16], the pressure induced superconductivity [17] and have potential applications in nanoscale devices due to their structure of tunnel type.

Previously, various kinds of sodium vanadium oxide based nanostructures such as nanowires, nanobelts, nanorods, nanotubes, etc. have been reported [16,18–23]. Nowadays more and more attention has been paid to ring-like nanomaterials due to their size, special morphology related properties and potential nanoscale applications. For example nanorings of ZnO [2], GaN [24], Ga_2O_3 [25], SnO [3], InGaN [26], BN [27] etc., were synthesized through a high temperature solid state reaction method. This method needs high temperature or special equipment or conditions. But solution-based methods are well-known for their advantages in tailoring the size and morphology of the nanostructures. Among which hydrothermal method has several advantages in terms of synthesis control: the control of parameters such as reaction temperature, pH and solvent concentration, as well as the addition of templates or additives, making it possible to obtain with different morphologies and structures in a simple manner. For instance, nanorings of CuO [8], Fe_2O_3 [1], CdS [28], PbS [29], etc. were prepared by hydrothermal method.

* Corresponding author at: Centre for Nano and Materials Science, Jain University, Jakkasandra Post, Kanakapura, India. Tel.: +91 80 2757 7250.
E-mail address: nagarajugn@rediffmail.com (G. Nagaraju).

0025-5408/$ – see front matter © 2012 Elsevier Ltd. All rights reserved.
http://dx.doi.org/10.1016/j.materresbull.2012.08.010

There are few reports particularly on vanadium oxide based nanorings synthesized by hydrothermal method. $Ag_2V_4O_{11}$ nanorings/microloops [4] were prepared using V_2O_5 and $AgNO_3$ at 170 °C for 12 h. VO_2 nanorings [30] were obtained using V_2O_5 sol in presence of excessive PEG-6000 at 200 °C for few days. Here PEG plays key roles in depressing the thickness and length of the VO_2 nanobelt that acts as a predecessor of the nanorings formation. $V_2O_5{\cdot}xH_2O$ nanorings/microloops [7] were synthesized using ammonium vanadate in presence of $Mg(NO_3)_2$ at 160–190 °C for 20–40 h. The driven force for nanorings and microloops formation is due to Mg^{2+} induced asymmetric strain on the V_2O_5 nanobelts. $Na_2V_6O_{16}{\cdot}3H_2O$ nanorings/nanoloops were prepared using Na_3VO_4 and Na_2CO_3 in acidic medium at 200 °C for 1 day [31]. In all the above cases added metal ions or surfactant plays a crucial role for the formation of nanorings. Interestingly our group has reported the synthesis of $(NH_4)_{0.5}V_2O_5{\cdot}mH_2O$ nanorings and triangles [6] at 160 °C for 2 days without using any surfactant, solvents, addition of foreign metal ions. This will minimize the impurity level.

Continuing our efforts on the synthesis of vanadium oxide based nanorings/nanobelts, we are the first to report the synthesis of $Na_{0.28}V_2O_5$ nanorings/nanobelts in aqueous acidic medium without using any surfactant, solvents, addition of foreign metal ions. To the best of our knowledge, no reports are available on the synthesis of $Na_{0.28}V_2O_5$ nanorings by any method. As expected, high yield nanobelts are formed due to the outward embodiment of the highly anisotropic internal structure, and then polarization induced self-coiling of nanobelts indeed gives $Na_{0.28}V_2O_5$ single crystalline nanoring structure. Further we have examined the electrochemical performance toward lithium battery.

2. Experimental

2.1. Synthesis

Hydrothermal process was carried out like our previous report to prepare ammonium vanadate nanorings/triangles [6]. 270 mg $NaVO_3$ was dispersed in 20 mL distilled water taken in a 30 mL capacity Teflon tube. CH_3COOH (pH ≈ 3) was added to it and stirred for 10 min. The resultant wine-red solution was subjected to hydrothermal treatment at 130–160 °C for 1–2 days. After the hydrothermal treatment, the autoclaves were cooled to room temperature naturally. The reddish-brown non-adherent spongy-like bulky material was collected from centrifugation and washed with distilled water and absolute alcohol for several times before being dried in oven.

2.2. Characterization

Powder X-ray diffraction data were recorded on Philips X'pert PRO X-ray diffractometer with graphite monochromatized Cu–Kα (1.5418 Å) radiation. The Fourier transform infrared spectrum of the sample was collected using Bruker Alpha-P spectrometer. Raman spectroscopic study was performed on Renishaw InviaRaman spectrometer with 628 nm He–Cd laser. The morphology of the product was examined by JEOL-JSM-6490 LV scanning electron microscope (SEM) and CM12 Philips transmission electron microscope (TEM) equipped with energy dispersive X-ray spectrometer (EDS).

3. Results and discussion

X-ray diffraction pattern of the samples (Fig. 1) prepared at 130–160 °C for 1–2 days is indexed as monoclinic $Na_{0.28}V_2O_5$. The calculated cell parameters for monoclinic $Na_{0.28}V_2O_5$ are a = 16.43 Å, b = 3.61 Å, c = 10.1 Å and β = 109.61° (space group C2/m) are in good agreement with the literature data [JCPDS no. 75-0544]. No other peaks from impurities were detected, indicating $Na_{0.28}V_2O_5$ is the only phase present.

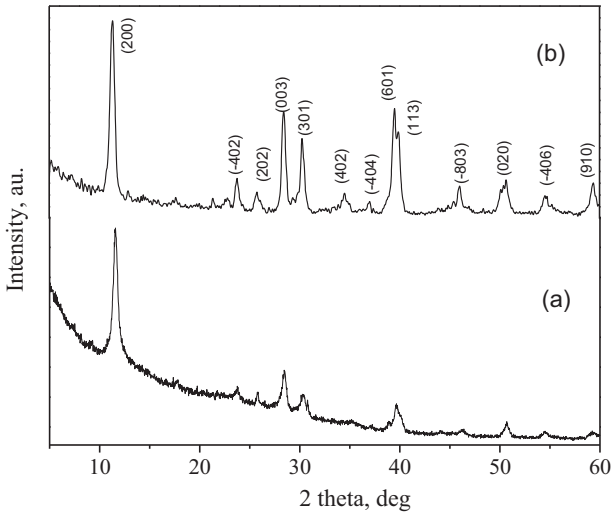

Fig. 1. XRD pattern $Na_{0.28}V_2O_5$ prepared at (a) 130 °C for 2 days and (b) 160 °C for 1 day.

In the FTIR spectrum of nanorings/nanobelts of $Na_{0.28}V_2O_5$ (Fig. 2), the vanadium–oxygen stretching vibrations appear in the range 400–1100 cm^{-1}. The band centered at 958 cm^{-1} is assigned to V=O stretching vibration, which is sensitive to intercalation and suggests that Na^+ ions are inserted between the vanadium oxide layers [32]. The splitting of this 958 cm^{-1} band into two absorption peaks at 946 and 996 cm^{-1} as compared to standard V_2O_5 (~1020 cm^{-1}) arises from the formation of two inequivalent V=O groups [6]. The bands at 946 and 996 cm^{-1} are respectively assigned to the V=O stretching of distorted octahedral and distorted square pyramids. The bands at 457, 715 and 825 cm^{-1} corresponding to the V–O–V symmetric stretch, asymmetric stretch and deformation modes, respectively. The band at 3584 and 1635 cm^{-1} is due to symmetric and bending vibration mode of absorbed water molecule on the surface [21,33].

The Raman spectrum of the $Na_{0.28}V_2O_5$ nanorings/nanobelts is as shown in Fig. 3. The spectrum shows clearly the modes located

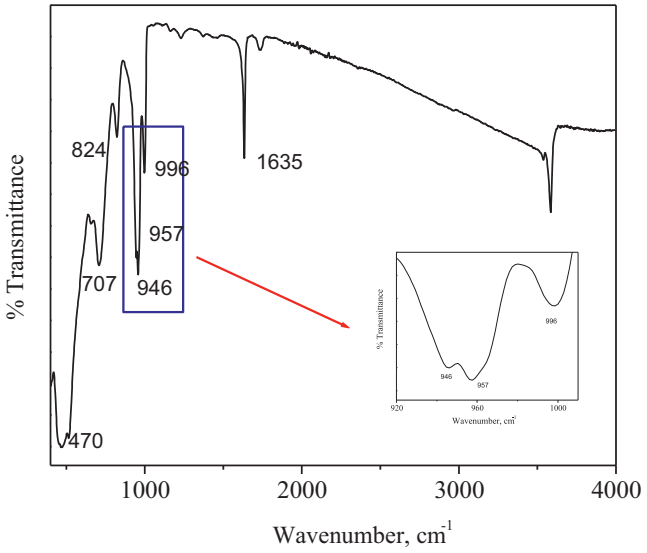

Fig. 2. FTIR spectrum of $Na_{0.28}V_2O_5$ nanoring/nanobelts prepared at 130 °C for 2 days.

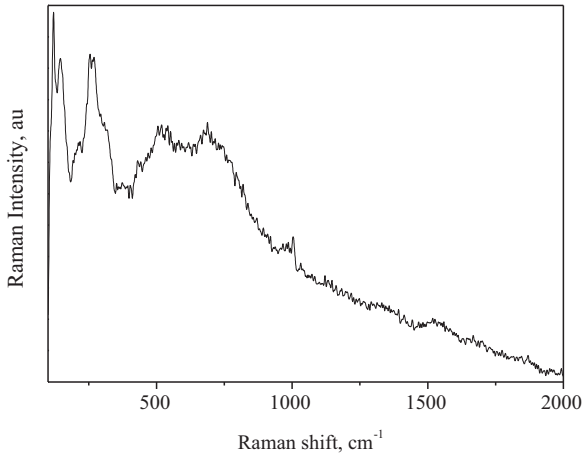

Fig. 3. Raman spectrum of $Na_{0.28}V_2O_5$ nanoring/nanobelts prepared at 130 °C for 2 days.

at 121, 144, 215, 261, 514, 688 and 1005 cm^{-1}. The bands below 400 cm^{-1} can be assigned to V–O and V–O–V bending modes, while the higher frequency modes originate from the stretching vibrations of the different V–O bonds in the $(V_1)O_6$, $(V_2)O_6$ and $(V_3)O_5$ polyhedra. The Ag symmetry modes are observed at 125, 215, 261, 511, 1002 cm^{-1} whereas Bg symmetry modes are evidenced at 146 and 687 cm^{-1}. The Ag symmetry modes observed at 511 cm^{-1} and 1002 cm^{-1} correspond to the V_3–O_7 and V_1–O_4 stretching vibration. The Bg symmetry mode observed at 687 cm^{-1} corresponds to the antisymmetric V_1–O_2–V_1 stretching vibration [20]. The results from XRD, FTIR and Raman studies confirm that the obtained nanorings/nanobelts are $Na_{0.28}V_2O_5$.

The morphology of the as obtained $Na_{0.28}V_2O_5$ nanorings/nanobelts prepared at different temperature and durations was examined by scanning electron microscopy. Fig. 4 shows SEM images of the $Na_{0.28}V_2O_5$ prepared at 130 °C for 1 day, where the dominant components are nanobelts and a significant amount of nanorings structures was observed. The as-synthesized sample was composed of many freestanding nanorings at a significant percentage (20–40%) of the yield and 70% reproducibility from run to run. We can clearly observe that the nanorings are made of nanobelts as well as nanowires. The nanorings made of nanobelts have a width of about 200–300 nm and thickness of about 60–100 nm. The rings have an inner diameter of about 1.5–3.5 μm and several tens of microns in length were observed. Nanorings made of nanobelts have a perfect circular shape with very smooth and flat surfaces. The inset of Fig. 4c and d shows clearly the joining of the two ends of the nanobelts to form nanorings.

Further increase in hydrothermal duration to 2 days at 130 °C, concentric nanorings made of nanobelts were observed (Fig. 5). The rings have a width of about 400–700 nm, thickness is around 100 nm, inner diameter of about 3–6 μm and several tens of micrometer in length were observed. Self-coiling of the polar nanobelts is evident, because nanorings diameter is below 1.0 mm. By careful observation, we can find the different stages of nanoribbon bending to produce nanorings without fracture. For 1 day nanorings formation starts and at 2 days uniform nanorings were observed. Further increase in hydrothermal duration to 3 days (Fig. S1), ring formation was not taken place and also nest structure gradually decreases.

With increase in hydrothermal treatment temperature to 160 °C for 1 day (Fig. 6), again we can observe the presence of nanorings. Here we can clearly distinguish two types of nanorings, i.e., nanorings made up of nanobelts as well as nanorods. Here the rings are looking like automobile tire (Fig. 6a) and tube (Fig. 6b). The width of the nanorings (Fig. 6a) is around 3 μm and inner diameter is around 9 μm. The thickness of the ring (Fig. 6b) is around 1.2 μm and the inner diameter is 3.5 μm. Further increase in hydrothermal duration to 2 days at 160 °C (Fig. S2), no nanorings were observed. From the above observation we concluded that ring formation takes place at 130 °C for 1–2 days and 160 °C for 1 day.

We have also examined the effect of calcination on the morphology of the nanorings/nanobelts. The nanorings were not destroyed even when the material is subjected to calcination at 300 °C for 2 h (Fig. S3). Decrease in temperature to 110 °C for 3 days also, no rings were observed (Fig. S4). We have also noticed that changing the precursors to ammonium vanadate, nanorings were not formed at 130 °C for 2 days (Fig. S5).

The morphology and structure of the nanorings/nanobelts were further characterized by TEM and selected area electron diffraction (SAED) patterns. Figs. 7 and 8 show the TEM images of the product prepared at 130 °C for 2 days and 160 °C for 1 day, respectively. Here also we can clearly observe that the nanorings are made of nanobelts as well as nanorods. The width of the nanorings is about 500 nm and thickness is about 100 nm. The nanorings made of nanorods possess 1–2 μm in thickness, inner diameter of about 5–7 μm. Figs. 4c and d and 7d(inset), suggest that nanorings are formed by joining the two ends of nanobelts. Each nanoribbon is uniform along their entire length of about 100–250 nm in width and several microns in length. The selected area electron diffraction pattern taken from a single nanobelt (inset of Figs. 7f and 8f) indicates that the nanobelts are single crystalline in nature. The microscopic elemental analysis of the selected nanorings and nanobelts is checked by energy dispersive X-ray spectroscopy (Fig. S6), which reveal the existence of Na, V and O elements.

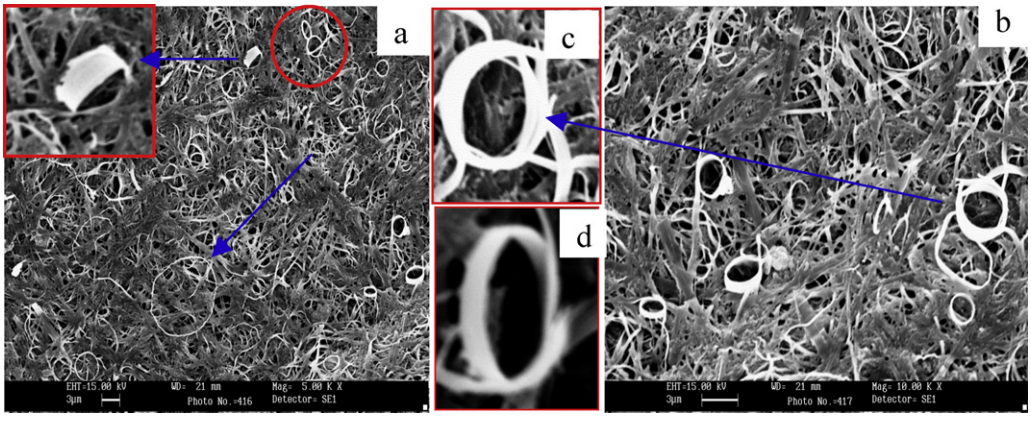

Fig. 4. SEM images of $Na_{0.28}V_2O_5$ nanoring/nanobelts prepared at 130 °C for 1 day.

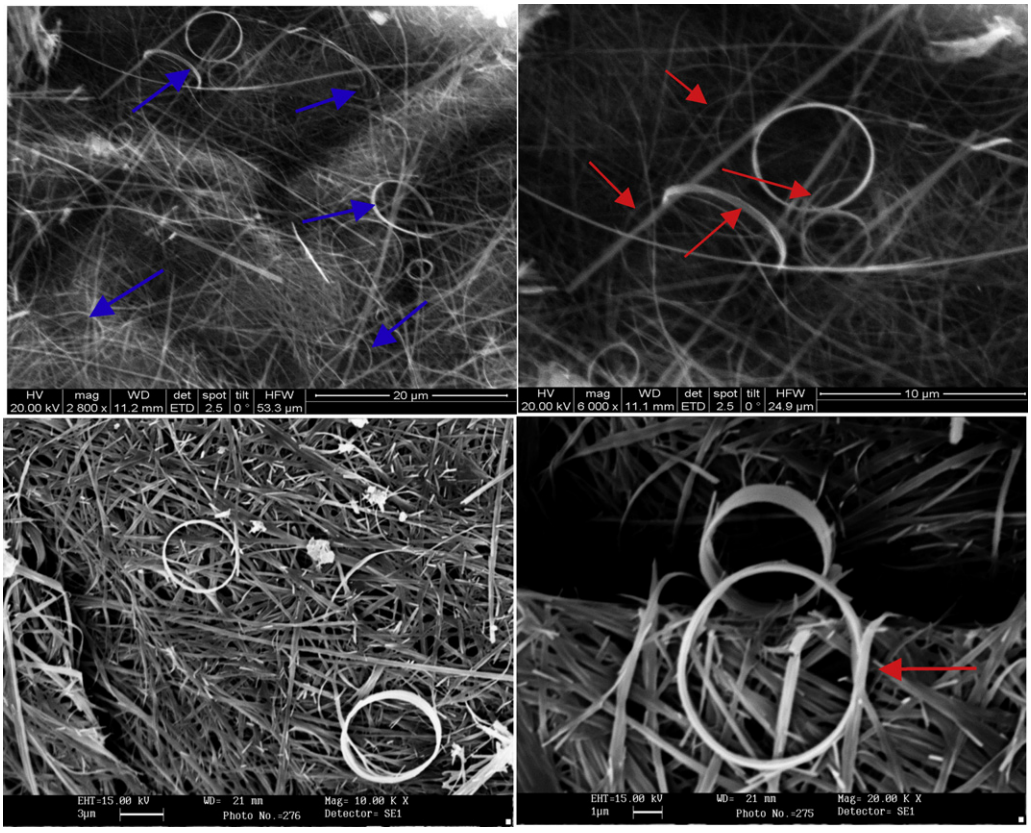

Fig. 5. SEM images of $Na_{0.28}V_2O_5$ nanoring/nanobelts prepared at 130 °C for 2 days.

3.1. Crystal growth and formation mechanism of $Na_{0.3}V_2O_5$ nanorings

The exact growth mechanism for the formation of these 1D nanobelts is still unclear. However, it is clear from the experimental data that the growth process does not involve a template-directed dependency nor is it related to the presence of additives or the solvents. Based on the results presented in our work, it seems that the nanowire growth mechanism is independent of the synthesis route adopted. In this experiment, there is a only a transformation of $NaVO_3$ to $Na_{0.28}V_2O_5$ is takes place in presence of acid. First sodium vanadate is dispersed in water followed by the addition of acid (pH ≈ 3). Decrease in pH causes instability of $NaVO_3$, giving rises to decavanadate species. This aqueous decavanadate solution is subjected to hydrothermal treatment, trivandate is formed. The obtained trivanadate reacts with the Na^+ where the vanadate chains (constructed by VO_6 octahedra and V_2O_8 units) linked by sharing the edges or the corners to form 3D framework structures, in which the sodium ions can accommodate these framework tunnels. As a result, these chain structures may contribute to the preferential growth of 1D nanobelt consistent with the sodium vanadate crystal structure. Two phases can actually be formed upon acidification of sodium metavanadate aqueous solutions namely NaV_3O_8 and $Na_xV_2O_5$. Their respective amounts depend on experimental conditions, pH, temperature, etc. Trivanadate is formed above pH 5 while below pH = 3.5, $Na_xV_2O_5$ is observed [34,35]. At very low pH, the formed trivanadate is further

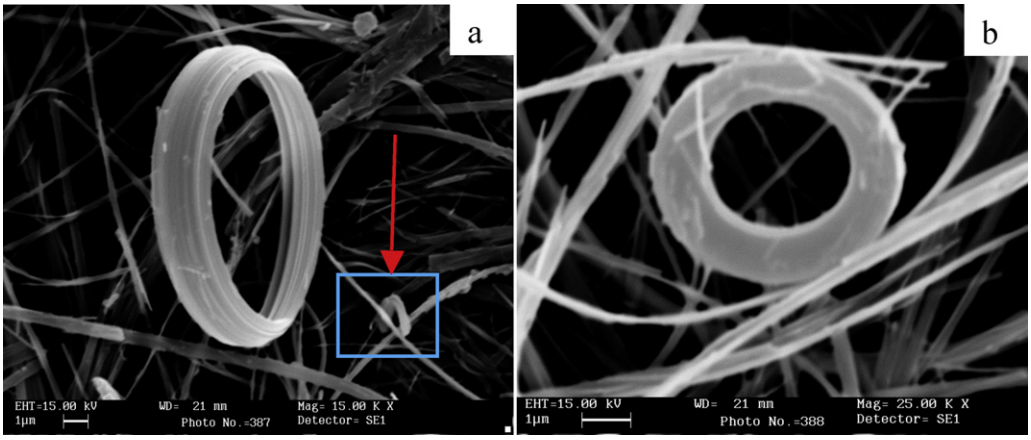

Fig. 6. SEM images of $Na_{0.28}V_2O_5$ nanoring/nanobelts prepared at 160 °C for 1 day.

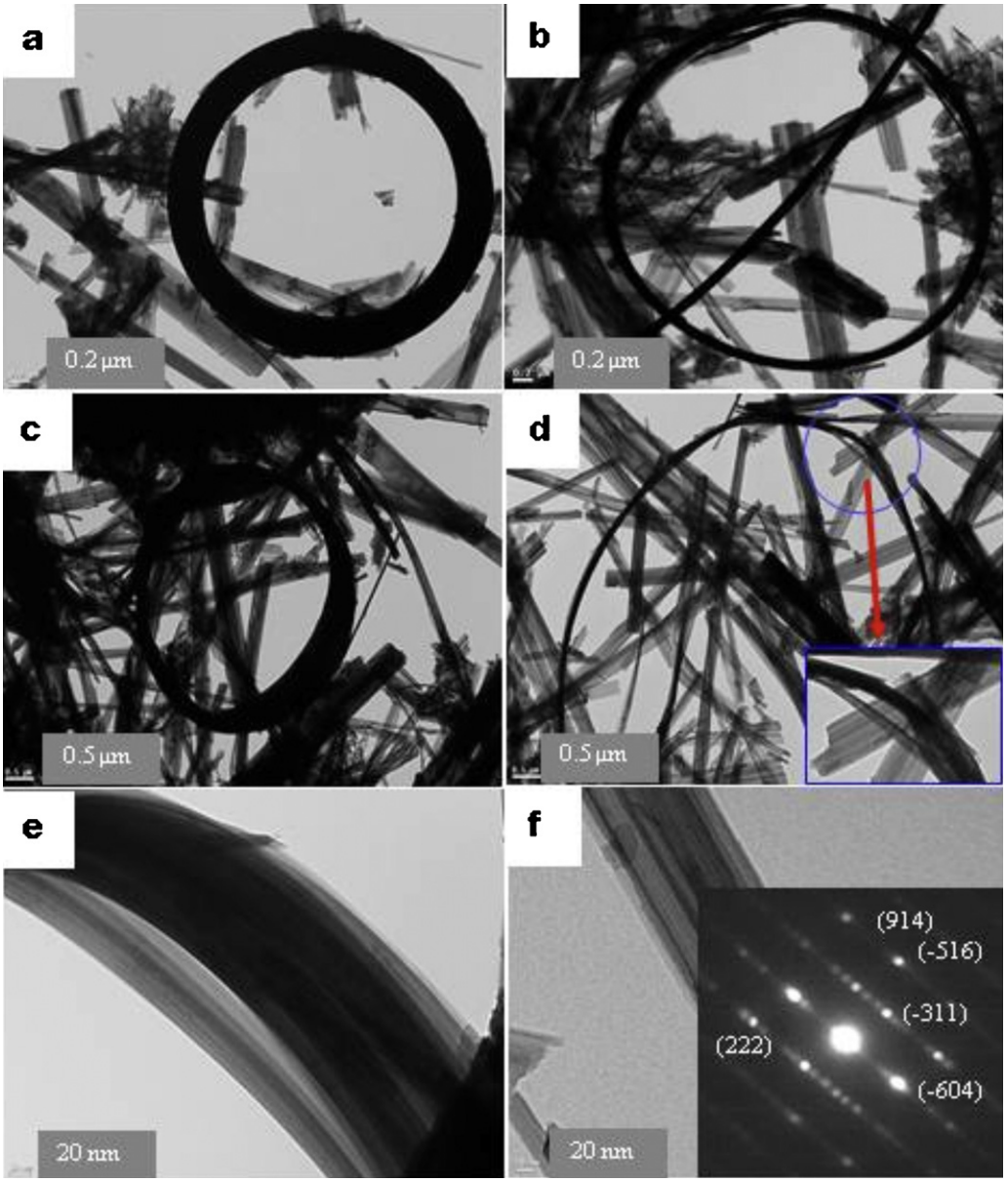

Fig. 7. TEM images of $Na_{0.28}V_2O_5$ nanoring/nanobelts prepared at 130 °C for 2 days.

reacts with H^+, leading to the formation of $Na_{0.28}V_2O_5$ nanorings/nanobelts.

$$NaVO_3 + CH_3COOH \rightarrow HVO_3 + CH_3COONa \quad (1)$$

$$10HVO_3 \rightarrow [H_2V_{10}O_{28}]^{4-} + 4H^+ + 2H_2O \quad (2)$$

$$3[H_2V_{10}O_{28}]^{4-} \rightarrow 10V_3O_8{}^{1-} + 1/2O_2 + 3H_2O \quad (3)$$

$$V_3O_8{}^{1-} + Na^+ \rightarrow NaV_3O_8 \quad (4)$$

$$24NaV_3O_8 + 14CH_3COOH \rightarrow 36Na_{0.28}V_2O_5 + 14CH_3COONa + 7H_2O + 5/2O_2 \quad (5)$$

Various mechanisms have been proposed to explain the growth of inorganic ring-like nanostructures. A cation induced (Mg^{2+}) coiling growth mechanism was suggested by Liu and Xue to describe the formation of $V_2O_5{\cdot}xH_2O$ nanorings and microloops [7]. $Cd(OH)_2$ nanorings were fabricated from $Cd(OH)_2$ nanoplates by ultrasonic chiseling [36]. In_2O_3 and Zn_2GeO_4 nanorings were synthesized through a kink induced structural evolution process from nanowires [37]. According to Liu and Zeng, CdS rings [28] were synthesized via the self-assembly of nanoparticles with an intrinsic hexagonal symmetry. Murray et al. proposed an oriented attachment mechanism of nanoparticles to explain the formation of PbSe nanorings [38]. Wang et al. proposed the loop-by-loop coaxial, uniradius, self-coiling of a single nanobelt in order to explain the formation of ZnO nanorings [2] in the vapor phase. A similar process was suggested by Shen and Chen for the synthesis of $Ag_2V_4O_{11}$ nanorings and microloops [4] from solutions. In a recent publication, we suggested a 'cation induced coiling growth mechanism' process for the formation of $(NH_4)_{0.5}V_2O_5{\cdot}mH_2O$ rings, triangles and ovals from solutions [6]. The same mechanism holds good to certain extent to explain the formation of $Na_{0.28}V_2O_5$ nanorings, because of the same monoclinic crystal structure.

The formation of nanobelts is a prerequisite for the further spontaneous self-coiling into the final nanoring structures. Our

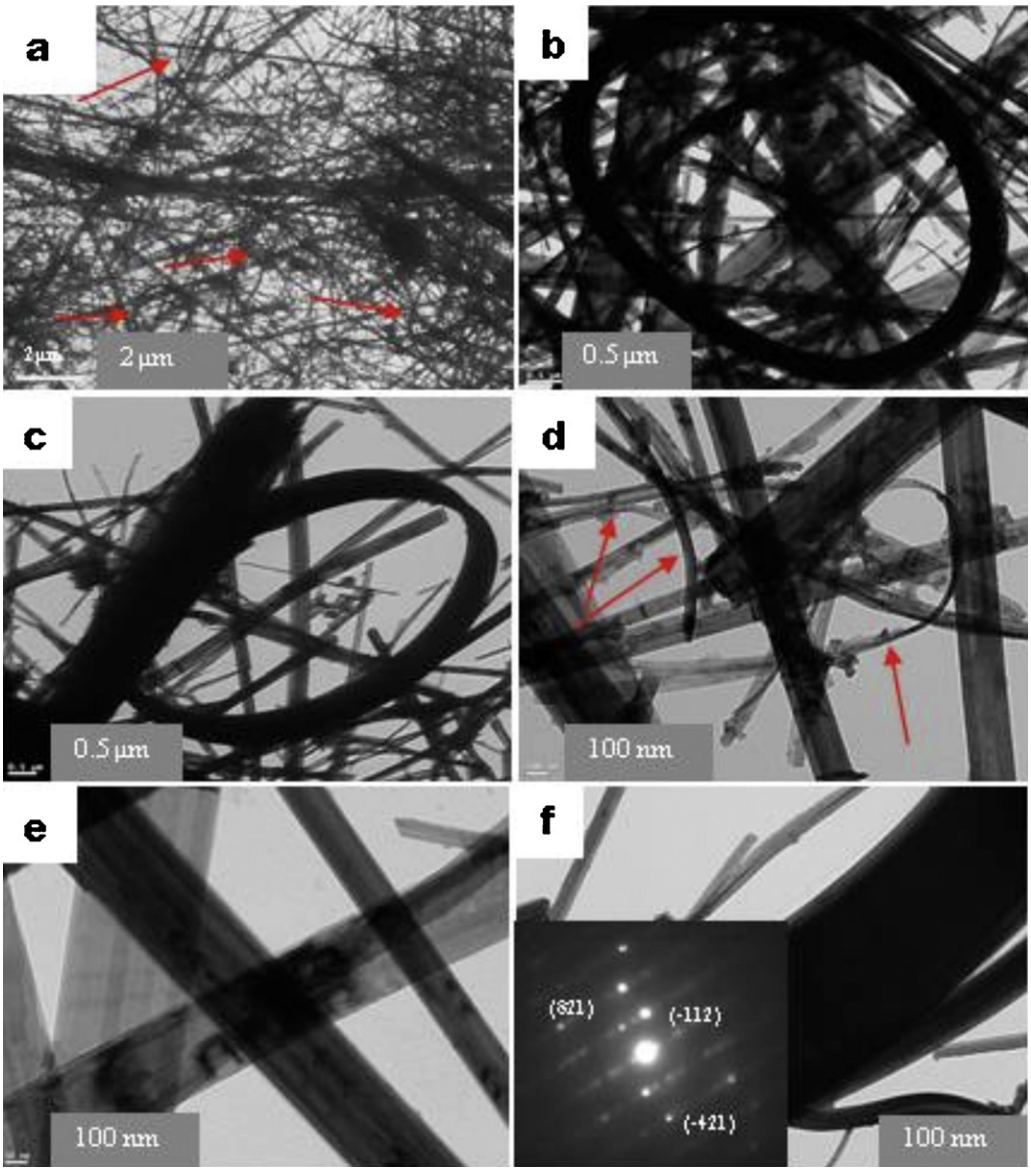

Fig. 8. TEM images of $Na_{0.28}V_2O_5$ nanoring/nanobelts prepared at 160 °C for 1 day.

solution-based synthesis strategy provides a way to directly obtain $Na_{0.28}V_2O_5$ nanobelts from a single source and the nature of nanobelts originates from the way its atoms are packed in the crystal structure.

As stated above $Na_{0.28}V_2O_5$ belongs to monoclinic crystal structure and contains tunnels formed by the association of VO_6 octahedra and VO_5 trigonal bipyramids frameworks along the *b*-axis. This leads to zigzag double chains composed of edge-sharing $(V_1)O_6$ octahedra and corner sharing $(V_2)O_6$ distorted octahedra as well as edge-sharing $(V_3)O_5$ squared-base pyramids. Each tunnel contains two equivalent interstial sites. Na^+ ions are distributed equally between the two interstial sites with the appearance of regular alteration of occupied and vacant sites. Because of this, $Na_{0.28}V_2O_5$ has a highly anisotropic crystal structure with the highest stacking density along *b*-axis. However, the double chains connected along the *c*-axis have loosed-pack tunnel structures, and considerably large interlayer distances along the *a*-axis, indicating the relatively lower stacking densities along the *a*- and *c*-axes. This shows that slower growth rates in these two directions.

Zhou groups have synthesized $Na_{0.28}V_2O_5$ nanowires in the presence of HSO_4^{1-} [19], Chandrappa et al. have synthesized $(NH_4)_{0.5}V_2O_5$ nanobelts/nanorings in the presence of citrate ion [6], Yu et al. have synthesized $Na_2V_6O_{16}{\cdot}3H_2O$ nanobelts in the presence of F^{-1} [39]. Avansi et al. have synthesized $Na_2V_6O_{16}{\cdot}nH_2O$ nanowires in presence of OH^{-1} [18], Liu et al. synthesized $V_2O_5{\cdot}xH_2O$ nanobelts/nanorings in presence of Mg^{2+} [7], Xue et al. synthesized $Na_2V_6O_{16}{\cdot}3H_2O$ nanobelts/nanorings and $(NH_4)_2V_6O_{16}{\cdot}5H_2O$ nanobelts/nanorings in presence of Na_2CO_3 [31]. All the above examples suggest that presence of anions or metal ions role is very crucial for the formation of nanobelts or nanorings.

To know the detailed mechanism we are considering $AgVO_4$ nanobelts/nanorings [40] in presence of pyridine as an example. They proposed that during the formation of nanobelts, pyridine plays an important role not only in stabilizing pH value but also in slowing the reaction because pyridine molecules can easily coordinate with silver ions to form pyridine salt. No nanobelts can be obtained, and instead aggregated particles are obtained in the absence of pyridine, which could be due to a too fast reaction speed.

With the above knowledge, we have also conducted the experiment using formic acid instead of acetic acid, and found that there is no formation of/nanobelts/nanorings at 130 °C for 2 days (Fig. S7). This clearly shows that role of acetate ion is very important during the formation of $Na_{0.28}V_2O_5$ nanorings/nanobelts. Acetic acid undergoes dissociation in water produces CH_3COO^- and H^+. The H^+ ions are maintaining the pH of the solution (pH ≈ 2) and CH_3COO^- may coordinate with the Na^+ or it adsorb selectively to the special crystal facets leading to the formation of flexible $Na_{0.28}V_2O_5$ nanobelts. The nanobelts have a quite large length–width (thickness) ratio. Thus a long structure easily causes bending due to surface charge, space charge or surface stress, resulting in considerable strains, which are common in nanobelts and nanowires [41].

Based on the thermodynamics aspect, we believed that the presence of residual/non intercalated ion such as Na^+ ions from the solution plays a vital role for the formation of ring structures, but the negatively charged ions such as CH_3COO^- behaves as a monodentate ligand. This ligand plays a crucial role in nanobelt formation as observed previously for the formation of sodium vanadate [39]. The structure of $Na_{0.28}V_2O_5$ can be described as an assembly of stacked V_2O_5 bilayers. Vanadium coordination is based on [VO_5] square pyramids with a short V=O double bond along the '*z*' axis perpendicular to the basal planes. Na^+ ions are intercalated between the vanadium oxide layers. The vanadium oxide layers exhibit a polar structure arising from the $V{=}O^{\delta-}$ perpendicular to the layer plane within the VO_5 square pyramids. Positively charged Na^+ ions can be attracted by the $V{=}O^{\delta-}$ dipoles on both sides of the bilayers. Moreover, Na^+ ions present inside the tunnels, in four interstitial equivalent sites per unit cell along the *b*-axis makes the vanadium oxide bilayers favor the flexibility of $Na_{0.28}V_2O_5$ nanobelts. 'According to the so-called 'cation-induced coiling' model, when the amount of residual Na^+ ions from the solution adsorb asymmetrically on both the top or the bottom surfaces of a thin, flexible $Na_{0.28}V_2O_5$ nanobelt, asymmetric strain energy is induced. When this asymmetric induced strain energy becomes larger than the elasticity energy, the flexible $Na_{0.28}V_2O_5$ nanobelt tends to self-coil into a circular ring.

3.2. Electrochemical properties

The electrochemical properties of the $Na_{0.28}V_2O_5$ nanoring/nanobelts were tested in Swagelok cells assembled in an argon filled glove box (Jacomex). The electrodes were made by mixing 70 wt.% active material ($Na_{0.28}V_2O_5$ nanoring/nanobelts), 20 wt.% conductive material (acetylene black) and 10 wt.% binder [poly(vinylene difluoride, PVDF]. The slurry prepared using 1-methyl-2-pyrrolidone as a solvent was coated on aluminum foil as a current collector, finally dried in the oven at about 120 °C for 1 day. Lithium metal was used as the counter and reference electrodes. The electrolyte was 1 M $LiPF_6$ in ethylene carbonate (EC) and dimethylene carbonate (DMC) (1:1, v/v). Cyclic voltammetry (CV) measurements were performed using CHI 660C (CH Instrument Electrochemical workstation) between 1.5 and 4.0 V vs. Li^+/Li at a scan rate of 0.5 mV s^{-1}. Galvanostatic discharge–charge measurements were performed on an Arbin BT-2000 battery tested between 1.5 and 4.0 V vs. Li^+/Li at a current density of 0.1 mA g^{-1}.

The typical cyclic voltammogram (CV) of the $Na_{0.28}V_2O_5$ nanorings/nanobelts is shown in Fig. 9. The voltammogram is carried out at a scan rate of 0.5 mV s^{-1} in the potential range from 4 to 1.5 V vs. Li/Li^+. The cathodic peaks appear at about 3.45 V, 3.1 V and 2.3 V are ascribed to the multistep lithium ion insertion process and anodic reversible peak appear at 3.1 V corresponding to the extraction behavior of lithium ions from the host $Na_{0.28}V_2O_5$ nanorings/nanobelts electrode materials. The insertion/extraction

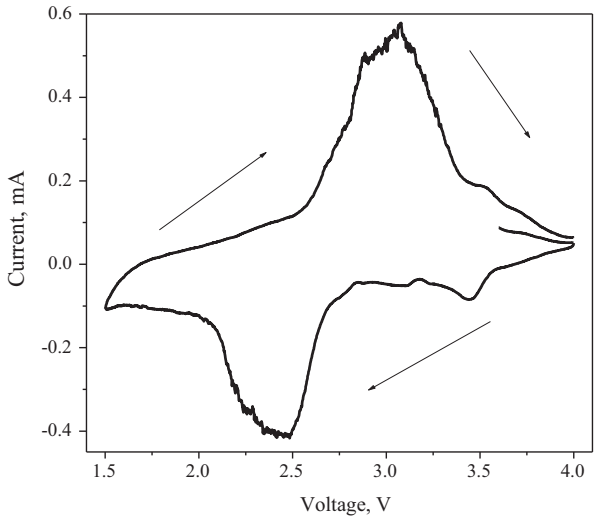

Fig. 9. Cyclic voltammogram of $Na_{0.28}V_2O_5$ nanorings/nanobelts prepared at 130 °C for 2 days.

behavior of lithium ions thus can be tentatively expressed as [16,43,44].

$$Na_{0.28}V_2O_5 + 0.33Li^+ + 0.33e^- \rightarrow Li_{0.33}Na_{0.28}V_2O_5 \quad \text{at} 3.45\,V \tag{6}$$

$$Li_{0.33}Na_{0.28}V_2O_5 + 0.33Li^+ + 0.33e^- \rightarrow Li_{0.66}Na_{0.28}V_2O_5 \quad \text{at} 3.1\,V \tag{7}$$

$$Li_{0.66}Na_{0.28}V_2O_5 + 1Li^+ + 1e^- \rightarrow Li_{1.66}Na_{0.28}V_2O_5 \quad \text{at} 2.5\,V. \tag{8}$$

Fig. 10 shows the discharge curves and the cycle performance for an electrode composed of $Na_{0.28}V_2O_5$ nanorings/nanobelts at a current density of 0.1 mA g^{-1}. The initial discharge capacity was found to be 320 mAh g^{-1} and even at after 69 cycles also it shows a specific discharge capacity of 175 mAh g^{-1}. We have also carried out the electrochemical performance of the products prepared at 130 °C for 1 day and 160 °C for 1 day and found that there is no much difference in the electrochemical discharge capacity of all the three products. The electrochemical behavior of the $Na_{0.28}V_2O_5$ is governed by the filling of specific available sites in the structure and is dependent on coulombic interactions between neighboring sites occupied by cations (Na–Li and Li–Li) [43]. The gradual decrease in discharge capacity with cycle no is explained as follows. In case of $Na_{0.28}V_2O_5$, Na^+ atoms in $Na_{0.28}V_2O_5$ are equally distributed between the two sites M_1 and $M_1{}^1$. Galy et al. [44] have shown that this bronze structure present two other possible tunnel structure, i.e., eight coordinated M_2 site and a tetrahedral M_3 site. All tunnels sites ore of the same symmetry. According to the four multiplicities of the sites and their half occupancy, one can suggest that the occupancy is easier the larger is the distance between an already occupied site and a vacant site. The first and second step lithium ion insertion gives a total alkali content of 0.63 and 1 could respond to half occupancy of the M_3 sites (at 3.45 V) and of the M_2 sites (at 3.1 V). Then by convince of symmetry when three sites are all half occupied, there is no occupancy of the third step lithium ion insertion. However the total occupancy of the three sites would corresponds to a smaller separation of the nearest neighbor sites of about 2 Å. Further insertion of Li ion at 2.45 V causes the lower reversibility. This indicate that electrochemical lithium insertion into sodium vanadium bronze is more reversible for $0 < x < 0.7$ than for higher lithium content [42]. The $Na_{0.28}V_2O_5$ monoclinic structure remains stable all along the Li insertion process, ie, for

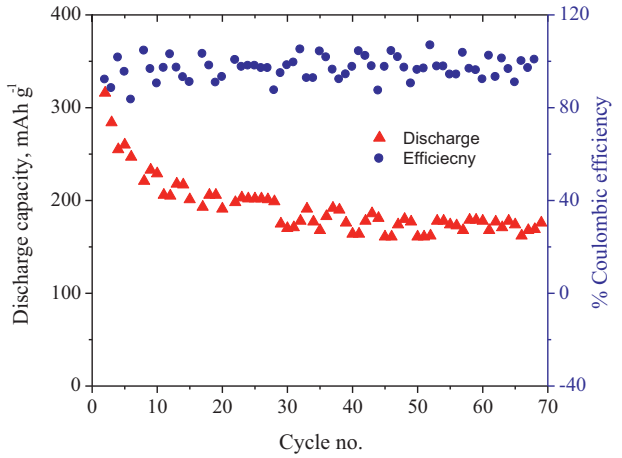

Fig. 10. Discharge capacity vs. cycle no. and Coulombic efficiency of $Na_{0.28}V_2O_5$ nanorings/nanobelts prepared at 130 °C for 2 days.

$0 < x < 1.6$ which makes this compound very attractive as rechargeable cathode material for lithium battery [45].

4. Conclusion

In conclusion, monoclinic phase of single crystalline $Na_{0.28}V_2O_5$ nanorings/nanobelts have been successfully synthesized by a simple low temperature hydrothermal method at 130–160 °C for 1–2 days without using any organics. The width of the nanorings is about 500 nm and thickness is about 100 nm. The nanorings made of nanorods possess 1–2 μm in thickness, inner diameter of about 5–7 μm. We have discussed the possible reason for the growth of sodium vanadium bronze nanobelts and the formation of nanorings. The as synthesized nanorings/nanobelts show an initial discharge capacity of 320 mAh g^{-1} and reaches to 168 mAh g^{-1} even after 70 cycles. The structure stability of this material during lithium insertion/extraction makes as a good cathode material for lithium ion battery.

Acknowledgement

One of the authors Nagaraju thanks to Prof. S. Sampath, Department of Inorganic and Physical Chemistry, Indian Institute of Science, Bangalore for providing electrochemical measurements.

Appendix A. Supplementary data

Supplementary data associated with this article can be found, in the online version, at http://dx.doi.org/10.1016/j.materresbull.2012.08.010.

References

[1] B. Lv, Y. Xu, D. Wu, Y. Sun, Chem. Commun. 47 (2011) 967.
[2] X.Y. Kong, Y. Ding, R.S. Yang, Z.L. Wang, Science 303 (2004) 1348.
[3] R. Yang, Z.L. Wang, J. Am. Chem. Soc. 128 (2006) 1466.
[4] G.Z. Shen, D. Chen, J. Am. Chem. Soc. 128 (2006) 11762.
[5] S. Ashoka, G. Nagaraju, G.T. Chandrappa, Mater. Res. Bull. 45 (2010) 1736.
[6] G.T. Chandrappa, P. Chithaiah, S. Ashoka, J. Livage, Inorg. Chem. 50 (2011) 7421.
[7] J. Liu, D. Xue, Nanoscale Res. Lett. 5 (2010) 1619.
[8] X. Wang, G. Xi, S. Xiong, Y. Liu, B. Xi, W. Yu, Y. Qian, Cryst. Growth Des. 7 (2007) 930.
[9] D. Yu, J.Q. Wu, Q. Gu, H.K. Park, J. Am. Chem. Soc. 128 (2006) 8148.
[10] M. Nath, B.A. Parkinson, J. Am. Chem. Soc. 129 (2007) 11302.
[11] J. Cao, J.L. Musfeldt, S. Mazumdar, N.A. Chernova, M.S. Whittingham, Nano Lett. 7 (2007) 2351.
[12] C.J. Patridge, C. Jaye, H. Zhang, A.C. Marschilok, D.A. Fischer, E.S. Takeuchi, S. Banerjee, Inorg. Chem. 48 (2009) 3145.
[13] G. Pistoia, M. Pasquali, G. Wang, L. Li, J. Electrochem. Soc. 137 (1990) 2365.
[14] S. Maingot, N. Baffier, J.P. Ramos, P. Willman, Solid State Ionics 67 (1993) 29.
[15] V. Manev, A. Momchilov, A. Nassalevska, G. Pistoia, M.J. Pasquali, J. Power Sources 54 (1995) 501.
[16] S. Sirbu, T. Yamauchi, Y. Ueda, P.H.M. Van Loosdrecht, Eur. Phys. J. 53 (2006) 289.
[17] T. Yamauchi, Y. Ueda, N. Mori, Phys. Rev. Lett. 89 (2002) 057002.
[18] W. Avansi, C. Ribeiro, E.R. Leite, V.R. Mastelaro, Mater. Chem. Phys. 127 (2011) 56.
[19] G.T. Zhou, X. Wang, J.C. Yu, Cryst. Growth Des. 5 (2005) 969.
[20] R.B. Hadjean, S. Bach, N. Emerya, J.P. Pereira-Ramos, J. Mater. Chem. 21 (2011) 11296.
[21] V.L. Volkov, G.S. Zakharova, N.V. Podvalnaya, M.V. Kuznetsov, Russ. J. Inorg. Chem. 53 (2008) 854.
[22] V.S. Reddy, I.H. Yeo, S. Mho, J. Phys. Chem. Solids 69 (2008) 1261.
[23] O. Durupthy, N. Steunou, T. Coradin, Maquet F J., C. Bonhomme, J. Livage, J. Mater. Chem. 15 (2005) 1090.
[24] J.K. Jian, Z.H. Zhang, Y.P. Sun, M. Lei, X.L. Chen, T.M. Wang, C. Wang, J. Cryst. Growth 303 (2007) 427.
[25] F. Zhu, Z.X. Yang, W.M. Zhou, Y.F. Zhang, Phys. Stat. Sol. (a) 203 (2006) 2024.
[26] Y. Wang, K. Zang, S. Chu, M.S. Sander, S. Tripathy, C.C. Fonstad, J. Phys. Chem. B 110 (2006) 11081.
[27] X. Hao, Y. Wu, J. Zhan, J. Yang, X.X. Xu, M. Jiang, J. Phys. Chem. B 109 (2005) 19188.
[28] B. Liu, H.C. Zeng, J. Am. Chem. Soc. 127 (2005) 18262.
[29] D. Yu, D. Wang, Z. Meng, J. Lu, Y. Qian, J. Mater. Chem. 12 (2002) 403.
[30] M. Li, F. Kong, Y. Zhang, G. Li, Cryst. Eng. Commun. 13 (2011) 2204.
[31] Y. Xue, X. Zhang, J. Zhang, J. Wu, Y. Sun, Y. Tian, Y. Xie, J. Mater. Chem. 22 (2012) 2560.
[32] H.F. Zhang, C.M. Wang, E.C. Buck, L.S. Wang, Nano Lett. 3 (2003) 577.
[33] H.L. Fei, M. Liu, H.J. Zhou, P.C. Sun, D.T. Ding, T.H. Chen, Solid State Sci. 11 (2009) 102.
[34] J. Livage, Chem. Mater. 3 (1991) 578.
[35] J. Livage, Coordin. Chem. Rev. 391 (1999) 190.
[36] J.J. Miao, R.L. Fu, J.M. Zhu, K. Xu, J.J. Zhu, H.Y. Chen, Chem. Commun. (2006) 3013.
[37] C. Yan, N. Singh, P.S. Lee, ACS Nano 4 (2010) 5350.
[38] K.S. Cho, D.V. Talapin, W. Gaschler, C.B. Murray, J. Am. Chem. Soc. 127 (2005) 7140.
[39] J.G. Yu, J.C. Yu, W.K. Ho, L. Wu, X.C. Wang, J. Am. Chem. Soc. 126 (2004) 3422.
[40] J.M. Song, Y.Z. Lin, H.B. Yao, F.J. Fan, X.G. Li, S.H. Yu, ACS Nano 3 (2009) 653.
[41] J. Wang, X.W. Sun, Z. Jiao, E. Khoo, P.S. Lee, J. Ma, H.V. Demir, Nanoscale 3 (2011) 4742.
[42] J.P. Pereira-Ramos, R. Messina, L. Znaidi, N. Baffier, Solid State Ionics 28–30 (1998) 886.
[43] M. Millet, J. Farcy, J.P. Pereira-Ramos, E.M. Sabbar, M.E. De Roy, J.P. Besse, Solid State Ionics 112 (1998) 319.
[44] J. Galy, J. Daniel, A. Casalot, J.B. Goodenough, J. Solid State Chem. 1 (1970) 339.
[45] J.P. Pereira-Ramos, R. Baddour, S. Bach, N. Baffler, Solid State Ionics 53–56 (1992) 701.